5-2017

High-content Screening of Clinically Tested Anticancer Drugs Identifies Novel Inhibitors of Human MRP1 (ABCC1)

Brian G. Perterson
South Dakota State University

Kee W. Tan
South Dakota State University, ktan097@gmail.com

Bremansu Osa-Andrews
South Dakota State University, bremansu@gmail.com

Surtaj H. Iram
South Dakota State University, surtaj.iram@sdstate.edu

Pharmacological Research 119 (2017) 313–326

Contents lists available at ScienceDirect

Pharmacological Research

journal homepage: www.elsevier.com/locate/yphrs

High-content screening of clinically tested anticancer drugs identifies novel inhibitors of human MRP1 (ABCC1)

Brian G. Peterson [1], Kee W. Tan [1], Bremansu Osa-Andrews, Surtaj H. Iram *

Department of Chemistry & Biochemistry, College of Arts and Sciences, South Dakota State University, Brookings, SD, USA

ARTICLE INFO

Article history:
Received 27 November 2016
Received in revised form 23 February 2017
Accepted 27 February 2017
Available online 28 February 2017

Chemical compounds studied in this article:
HS-173 (PubChem CID: 52936849)
TAK-733 (PubChem CID: 24963252)
Everolimus (PubChem CID: 6442177)
Cyclosporin A (PubChem CID: 5284373)
ESI-09 (PubChem CID: 6077765)
Deforolimus (PubChem CID: 11520894)
CX-6258 (PubChem CID: 44545852)
Tipifarnib (PubChem CID: 159324)
YM201636 (PubChem CID: 9956222)
AZD1208 (PubChem CID: 58423153)

Keywords:
MRP1
ABC transporter
High content imaging
Anti-cancer agent
Drug disposition
Drug-transporter interactions
Drug profiling

ABSTRACT

Multidrug resistance protein 1 (MRP1/ABCC1), an integral transmembrane efflux transporter, belongs to the ATP-binding cassette (ABC) protein superfamily. MRP1 governs the absorption and disposition of a wide variety of endogenous and xenobiotic substrates including various drugs across organs and physiological barriers. Additionally, its overexpression has been implicated in multidrug resistance in chemotherapy of multiple cancers. Here, we describe the development of a high content imaging-based screening assay for MRP1 activity. This live cell-based automated microscopy assay is very robust and allows simultaneous detection of cell permeable, non-toxic and potent inhibitors. The validity of the assay was demonstrated by profiling a library of 386 anti-cancer compounds, which are under clinical trials, for interactions with MRP1. The assay identified 12 potent inhibitors including two known MRP1 inhibitors, cyclosporine A and rapamycin. On the other hand, MRP1-inhibitory activity of tipifarnib, AZD1208, deforolimus, everolimus, temsirolimus, HS-173, YM201636, ESI-09, TAK-733, and CX-6258 has not been previously reported. Inhibition of MRP1 activity was further validated using flow cytometry and confocal microscopy for the respective detection of calcein and doxorubicin in MRP1-overexpressing cells. Among the identified compounds, tipifarnib, AZD1208, rapamycin, deforolimus, everolimus, TAK-733, and temsirolimus resensitized MRP1-overexpressing H69AR cells towards vincristine, a cytotoxic chemotherapeutic agent, by 2–6-fold. Using purified HEK293 membrane vesicles overexpressing MRP1, MRP2, MRP3, and MRP4, we also demonstrated that the identified compounds exert differential and selective response on the uptake of estradiol glucuronide, an endogenous MRP substrate. In summary, we demonstrated the effectiveness of the high content imaging-based high-throughput assay for profiling compound interaction with MRP1.

1. Introduction

The ATP-binding cassette (ABC) transporters represent a large evolutionarily conserved family of membrane proteins ubiquitous in practically all living organisms. In the human genome, a total of 48 ABC transporter genes have been identified and they are classified into seven subfamilies, designated A–G [1]. Functionally, ABC transporters are responsible for the transmembrane efflux of a remarkably broad spectrum of substrates, including ions, lipids, carbohydrates, peptides, and xenobiotics [1–3]. They are also well-known to regulate the absorption and disposition of various therapeutic agents [4,5]. The importance of these transporters is further underscored by the fact that mutations in ABC transporter genes are associated with human diseases, including Dubin–Johnson syndrome (ABCC2), pseudoxanthoma elasticum (ABCC6), cystic fibrosis (ABCC7), persistent hyperinsulinemic hypoglycemia of infancy (ABCC8), gout (ABCG2), intrahepatic cholestasis (ABCB4), schizophrenia (ABCA13), sitosterolemia (ABCG5 and ABCG8), and Tangier disease (ABCA1) [6,7]. Owing to their roles in regulating the absorption and disposition of various drugs, the US Food and Drug Administration (FDA) has recommended the investigation of interactions between drug candidates and a number of key ABC drug transporters [8]. Consequently, in the pharmaceutical industry, profiling of drug interactions with ABC drug transporters to determine a substrate/inhibitor relationship has become a standard component in the drug discovery process. This information can be used not only in the early discovery process to filter candi-

* Corresponding author at: Department of Chemistry & Biochemistry, College of Arts and Sciences, South Dakota State University, Avera Health Science Building, SAV-131, Box-2202, Brookings, SD, 57007, USA.
E-mail address: surtaj.iram@sdstate.edu (S.H. Iram).
[1] Equal contribution.

http://dx.doi.org/10.1016/j.phrs.2017.02.024

dates with undesirable interactions, but also during later stages of drug discovery including lead optimization and pre-clinical evaluation of compound toxicity and efficacy.

Multidrug resistance protein 1 (MRP1/ABCC1) is the second ABC transporter identified in humans and was originally discovered from a doxorubicin-selected drug-resistant lung cancer cell line [9]. In the human body, MRP1 is primarily expressed in the basolateral membrane of epithelial cells of organs such as the lung, gastrointestinal tract, kidney, pancreas, testis, placenta, bladder, and adrenal gland [10]. Consistent with its expression profile, MRP1 governs the absorption and disposition of a wide variety of endogenous and exogenous substrates across organs and physiological barriers, and serves to protect tissues from toxic molecules [11]. Notable physiological substrates of MRP1 include organic anions such as cysteinyl leukotriene (LTC_4), estradiol glucuronide ($E_2$17βG), glutathione (GSH), and cobalamin [12–14]. MRP1 may play a role in the pathogenesis of asthma and allergic reactions due to its ability to efflux LTC_4, a key pro-inflammatory signaling molecule [15]. In addition, MRP1 can also affect the bioavailability of various types of antivirals, antimalarials, and antibiotics [16].

MRP1, together with P-glycoprotein (P-gp/ABCB1) and breast cancer resistance protein (BCRP/ABCG2), is a major ABC transporter implicated in multidrug resistance (MDR), a phenomenon characterized by the resistance of malignancies to structurally and mechanistically distinct anti-cancer agents [17]. The involvement of MRP1 in MDR is consistent with the observation that MRP1 accommodates the efflux of conventional cytotoxic anti-cancer agents, such as doxorubicin, etoposide, vincristine, and methotrexate, as well as other newly developed anti-cancer agents that target specific signaling pathways such as tyrosine kinase inhibitors [16]. Overexpression of MRP1 has been linked to MDR in breast, lung, and prostate cancers, and several types of leukemia [18–21]. In addition, MRP1 overexpression has been shown to be predictive of poor clinical outcome in soft tissue sarcoma of limbs and trunk wall and primary neuroblastoma [22,23]. Interestingly, MRP1, together with MRP3 and MRP4, has also been implicated in the progression of neuroblastoma through functions other than their efflux of cytotoxic drugs [24].

Many *in vitro* assay systems have been developed to study drug interactions with ABC transporters, typically using cell lines overexpressing the transporter of interest or membrane vesicles prepared from these [25]. One of the widely used methods for high throughput screening of compound interaction with ABC transporter is the cell-based accumulation or efflux assay that utilizes a fluorescent substrate to probe if a test compound inhibits the efflux of the substrate by an ABC transporter. Flow cytometry or fluorescent plate reader are commonly used for the downstream fluorescence quantification [26–29]. Fluorescence detection with flow cytometry is generally more sensitive than fluorescent plate reader, which is commonly limited by a narrow detection range and high non-specific fluorescence background, and is typically more suited for assays performed in a homogenous condition [30]. The use of flow cytometry, on the other hand, usually involves cell washing and acquisition procedures that are more time-consuming and thus less compatible with a high throughput setup. Another commonly used assay for screening measures the uptake of a radiolabeled substrate into inside-out membrane vesicles expressing the transporter of interest. This type of assay is not compatible with intact cells and therefore cannot test the permeability of the compounds of interest. In recent years, image-based high content screening employing automated microscope platform has gained increasing use in biomedical research due to its capability to provide *in situ* visual data and to simultaneously study multiple biological targets [31]. Such strategy has recently been adapted for the high content imaging-based efflux assay as a superior alternative to flow cytometry- and fluorescent plate reader-based screening of compound interaction with P-gp and BCRP [32,33].

In this study, we describe the development, optimization, and validation of a high content imaging-based efflux assay to profile drug interactions with MRP1. The assay is performed in live cells and can be used to obtain information about modulation of target activity, toxicity and autofluorescence of the test compounds. The effectiveness of this assay is demonstrated by screening a unique library of 386 anti-cancer compounds currently under clinical trials targeting 12 types of cancers. The screening process identified 12 potent inhibitors including cyclosporine A and rapamycin, both of which are known inhibitors of MRP1. We validated the inhibitory activity of the positive hits using established methods widely used for ABC transporter studies and identified several anti-cancer agents that have not been previously known to inhibit MRP1. The ability of selected anti-cancer agents to reverse drug resistance in an MRP1-overexpressing MDR cell line is also demonstrated.

2. Materials and methods

2.1. Chemicals

Calcein-AM was purchased from Corning Life Sciences (Corning, NY). MK571 was acquired from Cayman Chemical (Ann Arbor, MI). Adenosine monophosphate (AMP), adenosine triphosphate (ATP), doxorubicin, estradiol 17-(β-D-Glucuronide) ($E_2$17βG), poly-D-lysine, thiazolyl blue tetrazolium bromide (MTT) were procured from Sigma-Aldrich (St. Louis, MO). [6,7-^{3}H]$E_2$17βG (49.9 Ci mmol^{-1}) was purchased from PerkinElmer (Waltham, MA). An anti-cancer compound library consisting of 386 anti-cancer small molecules under clinical trials for 12 different types of cancers was procured from Selleck Chemicals (Houston, TX).

2.2. Cell lines and cell culture

H69, H69AR, and HEK293 cells were obtained from ATCC (Manassas, VA). HEK293T cells were kindly provided by Dr. Adam Hoppe (South Dakota State University, Brookings, SD). HEK293/pcDNA3.1 and HEK293/MRP1 cells were kindly provided by Dr. Suresh V. Ambudkar (NIH, Bethesda, MD) and maintained as previously described (Muller et al., 2002). HEK293 and H69 cell lines were cultured in DMEM (GE Healthcare, Marlborough, MA) and RPMI 1640 (ATCC), respectively, supplemented with 10% fetal bovine serum. Cells were grown in a humidified incubator maintaining 5% CO_2 at 37 °C. H69AR cells were challenged monthly with 0.8 μM doxorubicin and cultured drug-free for one week before use.

Using pTagRFP-N vector as a backbone, we generated a new two-color human MRP1 construct using the similar cloning strategy as described before [58]. A stop codon was introduced after the MRP1 coding sequence into the two-color MRP1 construct to generate GFP-MRP1 (Green fluorescent protein fused with MRP1). Two-color MRP1 and GFP-MRP1 expression vectors were transfected into HEK cells (Agilent, Santa Clara, CA) using jetprime transfection reagent (VWR) according to the manufacturer's instructions. After 24 h, standard medium was replaced with medium containing G418 (400 ug/ml). Cells were maintained under G418 selection for two weeks. Then, the G418 amount was increased to 800 ug/ml. GFP expressing cells were sorted from the non-expressing cells using flow cytometry and maintained under G418 selection of 200 ug/ml.

2.3. MRP1 inhibition screening with automated image acquisition and analysis

Initial assay development and optimization were performed in H69 and H69AR cells with calcein-AM as the fluorescent substrate and MK571 as the positive control for MRP1 inhibition. Screening of

MRP1 inhibitors within the anti-cancer compound library was carried out using H69AR cells in 96-well Optical-Bottom Plates with Polymer Base (ThermoFisher Scientific, Waltham, MA) coated with poly-D-lysine (Sigma-Aldrich, St. Louis, MO). Cells were seeded at 6×10^4 cells per well in 100 μL culture medium and incubated overnight. At the onset of drug treatment, culture medium was removed and replaced with 80 μL of serum-free medium. Pretreatment was performed by adding 10 μL of test compounds (10 μM final concentration), DMSO (0.2% final concentration) as negative control, or MK571 (50 μM final concentration) as positive control. After 30 min, 10 μL of calcein-AM (0.25 μM final concentration) was added and the cells were incubated for 1 h. At the end of the incubation period, treatment was removed and the cells were washed once with PBS before 100 μL PBS containing 10 mM HEPES and 4.5% glucose was added.

Bright-field and fluorescent images (233.28 × 233.28 μM) were captured using an ImageXpress Micro XLS Widefield High-Content Analysis System (Molecular Devices, Sunnyvale, CA) equipped with a 0.70 numerical aperture 60 × objective. For each well, 4 bright-field and 4 fluorescent images were taken. Fluorescent images were acquired using a FITC filter with excitation and emission wavelengths of 482/35 and 536/40 nm, respectively, with an exposure time of 100 ms. It takes approximately 15 min to scan an entire plate. As the intracellular accumulation of calcein slowly dropped over time after treatment was removed, one negative and one positive controls were included in every two columns of the plate. Automated image analysis on fluorescent images was performed using the MetaXpress software (version 5.10.41, Molecular Devices). Segmentation of fluorescent objects on the FITC channel was carried out using a custom application module based on the 'Find Blobs' module. The custom module identifies fluorescent objects above a background fluorescent intensity and applies segmentation masks based on set parameters for object size. Three independent screening experiments were performed.

2.4. Flow cytometry-based calcein accumulation assay

H69 and H69AR cells were prepared in serum-free culture medium to a density of 7×10^5 cells/mL. The assay was performed by incubating 1 mL of cells with test compounds at 37 °C for 10 min before the addition of 25 nM calcein-AM. The final concentration of DMSO was 0.2% (v/v). Calcein incubation was performed for 30 min. The reaction was stopped by adding 3 mL of ice-cold PBS buffer. The cells were collected, washed again with PBS, and resuspended in ice-cold PBS containing 1% paraformaldehyde. Cell fluorescence was detected using a BD Accuri C6 flow cytometer (BD Biosciences, San Jose, CA). Excitation and emission wavelengths used were 480 and 533/30 nm, respectively. Fluorescence intensity was expressed as the mean value of 10,000 events. Treatments were performed in duplicate.

2.5. Doxorubicin accumulation assay

HEK293T cells were plated on poly-D-lysine-coated cover glass placed in a 6-well plate at a density of 3×10^5 cells/well in 2 mL culture medium. The next day, MRP1-GFP expression vector was transiently transfected into HEK293T cells using jetPRIME Transfection Reagent (Polyplus-transfection SA, Illkirch, France) according to the manufacturer's instructions. After 24–48 h, cells were pre-treated with 10 μM test compound for 30 min, followed by doxorubicin treatment (10 μM) for 1 h. Confocal microscopy was performed using a iMIC digital microscope (TILL Photonics GmbH, Gräfelfing, Germany) equipped with a 1.35 numerical aperture 60× oil-immersion objective. Excitation was performed at 488 nm for GFP and doxorubicin, with emission bands of 475/42 and 605/64 nm, respectively. Images were processed using ImageJ (NIH, Bethesda, MD).

2.6. Resistance reversal assay

Sensitivity of H69 and H69AR cells to vincristine and the ability of test compounds to reverse the resistance of H69AR cells against vincristine were analyzed using the MTT colorimetric assay. Cells were seeded in 96-well plates (CellBIND®, Corning) at 2.5×10^4 cells per well in 100 μL culture medium. After 24 h, 50 μL of test compound at selected concentration prepared in culture medium was added to the cells. After 1 h, 50 μL of vincristine at varying concentrations was added to the cells. Final DMSO concentration was at 0.5%. Cells were incubated for 96 h. At the end of the incubation period, 100 μL of culture medium was carefully removed and cells were treated with MTT (0.45 mg/mL) for 4 h. The formazan crystals were dissolved by the addition of 100 μL 15% SDS containing 10 mM HCl and absorbance at 570 nm were recorded using a Hidex Sense Beta Plus plate reader (Turku, Finland). Treatments were performed in triplicate.

2.7. Membrane vesicle preparation

Membrane vesicles were prepared as previously described with modifications [34]. Membrane vesicles were prepared from stable (HEK293/MRP1 and HEK293/MRP3) or transiently transfected (HEK293T/MRP2 and HEK293T/MRP4) cell lines. Cell pellets frozen at −80 °C were thawed and resuspended in buffer containing 50 mM Tris.HCl, pH 7.4, 250 mM sucrose, 0.25 mM $CaCl_2$, and 1× complete protease inhibitors (Santa Cruz Biotechnology, Dallas, TX), and then disrupted by nitrogen cavitation at 450 psi for 5 min. The lysates were supplemented with 1 mM EDTA and centrifuged at 500 × *g* at 4 °C for 10 min. The supernatant was collected and the cell pellet was resuspended and centrifuged again to collect the second supernatant. Pooled supernatant was layered over 35% (w/w) sucrose containing 10 mM Tris.HCl, pH7.4, and 1 mM EDTA and centrifuged at 25,000 rpm at 4 °C for 1 h in a SW28 rotor (Beckman Coulter, Brea, CA). The opaque membrane interface was collected and washed twice by ultracentrifugation. The membrane pellet was resuspended in transport buffer (50 mM Tris.HCl, pH 7.4, and 250 mM sucrose) and passed 20 times through a 27-gauge needle for vesicle formation. Protein concentration was determined using Quick Start Bradford Protein Assay (BioRad, Hercules, CA).

2.8. Membrane vesicular transport assay

ATP-dependent transport of [^{3}H]$E_2$17βG into the inside-out membrane vesicles was measured by a rapid filtration technique [34]. MRP-enriched membrane vesicles (2 μg protein) were incubated with 400 nM/20 nCi [^{3}H]$E_2$17βG for 1 min (MRP1) or 400 nM/50 nCi [^{3}H]$E_2$17βG for 5 min (MRP2-4) in a 30-μL reaction mixture containing 4 mM AMP or ATP, 10 mM $MgCl_2$, and test compound in transport buffer (250 mM sucrose and 50 mM Tris-HCl, pH 7.4). Reactions using MRP2-4 membrane vesicles also contained 10 mM creatine phosphate and 100 μg/mL creatine phosphokinase for ATP regeneration. Final DMSO concentration in the reaction was 0.29%. Reaction was stopped by adding ice-cold transport buffer. The resulting mixture was transferred to a 96-well MultiScreen$_{HTS}$-FB plate (EMD Millipore, Billerica, MA). Under vacuum aspiration, filter membranes were washed with 4 × 200 μL ice-cold suspension buffer. Radioactivity retained on the membranes was measured using a Tri-Carb 4810TR liquid scintillation counter (PerkinElmer, Waltham, MA). Treatments were performed in triplicate. ATP-dependent uptake was calculated by subtracting the uptake in the presence of AMP from the uptake measured in the presence of ATP.

2.9. Fluorescence spectroscopy

Fluorescence spectroscopy experiments were carried out using the Fluorimeter Model FL3-11 (HORIBA Edison, New Jersey). Membrane vesicles were prepared from stably transfected HEK293 cells expressing either GFP-MRP1 (donor control containing only GFP) or two-color MRP1 (containing both GFP and RFP fused to MRP1). Steady-state fluorimetry was employed for ligand-free (apo) and ligand-induced intramolecular fluorescence resonance energy transfer (FRET) analysis using experimental conditions described by (Verhalen et al., 2011) with modifications. Membrane vesicles (10 μg) in Tris sucrose buffer (250 mM Tris, 50 mM sucrose, pH 7.4) were prepared and pre-incubated with 10 μM of test compounds for 20 min at 37 °C in a water bath prior to spectroscopy experiment. GFP excitation was accomplished at 480 nm and RFP was excited at 530 nm. Emission for both GFP and RFP with integration time of 3 s was recorded at 480–650 nm. Emission scan of the donor only (GFP-MRP1 sample) was first collected while monitoring average donor emission peak intensity. Emission scan was then collected in the apo condition (ligand-free two-color MRP1); donor quenching was monitored and the average donor emission peak intensity was recorded. The test compound conditions were similarly scanned and donor quenching monitored. Each emission scan was collected at an interval of 5 nm every 3 s for a total of 10 min. Experiments were performed in triplicates. The relative fluorescence of the donor in the presence and absence of the acceptor was used to analyze data. The ratio of the average donor emission peak intensity (in counts per second, cps) in the donor-acceptor sample (two-color MRP1) to the average donor emission peak intensity in the donor only control (GFP-MRP1) was used to calculate the FRET efficiency of apo and compound-induced conditions.

2.10. High-content screening data analysis

The MetaXpress software provides the average fluorescence intensity value for each well, which is calculated from the fluorescence intensity values collected from the generated segmentation masks in the 4 captured images. The relative inhibition of each test compound on calcein-AM efflux was determined for each well using the following equation:

$$\%inhibition = \frac{X_T - X_{calcein-\mathrm{AM}}}{X_{MK-571} - X_{calcein-\mathrm{AM}}} \times 100,$$

where X represents the average fluorescence intensities and T represents the test compound. Positive and negative controls were placed in every two columns and used for the determination of the percent inhibition for compounds within the same columns. The Z'-factor, a parameter commonly used to reflect assay performance [31], was determined with the following equation:

$$Z'\text{-}factor = 1 - \frac{3\,(\sigma_{MK-571} + \sigma_{calcein})}{|\mu_{MK-571} - \mu_{calcein}|},$$

where σ and μ denote the standard deviations and means, respectively.

2.11. Statistical analysis

Statistical analyses were performed using IBM SPSS Statistics 19 (IBM, Armonk, NY). The differences between mean values were analyzed using linear mixed model analysis. Sidak correction was applied for multiple comparisons. Statistical testing was performed at 5% level of significance.

3. Results

3.1. Assay development and optimization

With ImageXpress High-Content Screening System, calcein-AM was used as a substrate for developing an imaging-based high-throughput screening efflux assay for MRP1. The H69AR cell line, which is a doxorubicin-selected MDR lung cancer cell line that expresses high levels of MRP1 [9], and its parental H69 cell line, were used for the development of this assay. Calcein-AM is a cell permeable and nonfluorescent compound that turns into highly fluorescent molecule after the acetoxymethyl ester (AM) moiety is cleaved off by cellular esterases. Calcein-AM is a well-known substrate for MRP1 and P-glycoprotein. In contrast to P-gp, MRP1 can also efflux the fluorescent anionic free calcein. The basic concept is that cells with no or very low expression levels of endogenous MRP1 and other transporters capable of effluxing calcein are expected to accumulate high levels of fluorescent calcein. In contrast, cells over-expressing MRP1 will show no or very little fluorescent calcein accumulation under similar experimental conditions due to active calcein efflux. For the quantification of fluorescence intensities in acquired images, we used a custom module in the MetaXpress software, which identifies cells by object segmentation on the FITC channel. Fig. 1 illustrates representative brightfield, fluorescent, and segmentation mask images of H69AR cells treated with calcein-AM. The MetaXpress software provides various built-in custom modules for object-based segmentation. Among the available custom modules, we selected the 'Find Blobs' module as the optimum module after manually comparing (1) the fitness and robustness of segmentation masks and (2) the processing time required to analyze data collected from one plate.

The strategy for the screening assay was to identify the conditions where H69AR cells would show little or no fluorescent substrate accumulation inside the cells due to efflux activity of the transporter. In contrast, high fluorescent substrate accumulation would be expected with MRP1 inhibition. To optimize the assay conditions for MRP1 using calcein-AM as substrate, we tested a range of calcein-AM concentrations (1 nM–1000 nM) and incubation times (30–180 min) using both parental H69 and MRP1-overexpressing H69AR cells. As shown in Fig. 2A, H69 cells show much higher fluorescence accumulation with increasing substrate concentration as compared with H69AR cells. To test if the difference observed between the two cell lines is specifically due to MRP1 efflux activity, effect of MK571 (a well-known MRP1 inhibitor) was observed at different calcein incubation times. As shown in Fig. 2B, there is no significant difference in calcein accumulation with or without MK571 in H69 cells at any calcein incubation time point. In contrast, MRP1-overexpressing H69AR cells exhibited high calcein accumulation with MK571 treatment compared with untreated H69AR cells at all calcein incubation time points (Fig. 2C). These data demonstrate the feasibility of using H69AR cells to develop a robust assay for high-throughput screening to identify inhibitors of MRP1 using calcein-AM as substrate.

3.2. Anti-cancer compound library screening for MRP1 inhibitors

Having successfully developed and optimized the high-content imaging-based assay, we sought to identify MRP1 inhibitors within a library of 386 anti-cancer small molecules under clinical trials for 12 different types of cancers. We screened the library using H69AR cells and calcein-AM as substrate. Screening was performed in the 96-well format in three independent experiments. Treatment with MK571 (50 μM) was used as 100% inhibition for calculating percent inhibition for the test compounds. As shown in Fig. 3, the relative MRP1-inhibitory activities of each anti-cancer agent from three experiments were plotted as a 3D scatter graph. We defined a

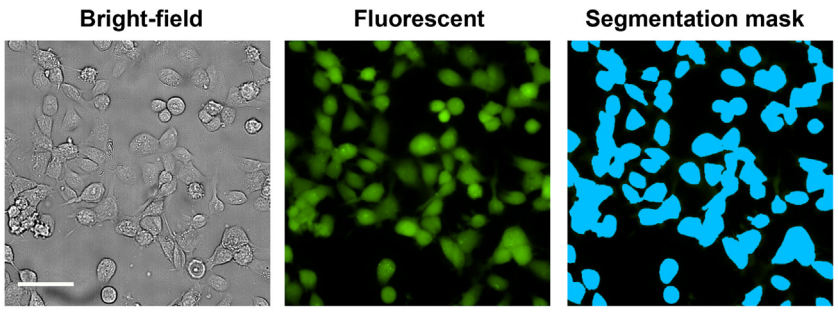

Fig. 1. Imaging-based detection of calcein accumulation. H69AR cells were treated with 0.25 μM calcein-AM and 50 μM MK571 for 1 h. Bright-field and fluorescent images were acquired using the ImageXpress Micro XLS Widefield High-Content Analysis System. Segmentation masks were generated using the MetaXpress software. Bar = 50 μm.

Table 1
Chemotherapeutic targets, % inhibition, and IC_{50} values for calcein accumulation inhibition for identified MRP1 inhibitors.

Compound	Chemotherapeutic Target	% Calcein Control Inhibition[a]	IC_{50}[b] (μM)
MK-571		100.0 ± 0	8.4 ± 1.8
Tipifarnib (Zarnestra)	Transferase	199.1 ± 56.8	3.7 ± 0.4
AZD1208	Pim	145.7 ± 25.3	0.7 ± 0.2
Rapamycin (Sirolimus)	Autophagy	142.5 ± 12.2	2.8 ± 0.5
Deforolimus (Ridaforolimus)	mTOR	111.9 ± 19.4	4.9 ± 0.9
HS-173	PI3K	94.0 ± 21.8	4.6 ± 1.5
YM201636	PI3K	81.9 ± 4.9	2.0 ± 0.2
ESI-09		74.6 ± 11.8	3.4 ± 0.1
Everolimus (RAD001)	mTOR	72.6 ± 7.8	2.6 ± 0.1
TAK-733	MEK	67.4 ± 12.7	8.5 ± 1.2
CX-6258	Pim	57.1 ± 16.4	[c]
Cyclosporin A		50.2 ± 2.7	6.6 ± 1.7
Temsirolimus (Torisel)	mTOR	43.3 ± 4.2	5.6 ± 0.1

[a] Mean ± SEM of n = 3 independent experiments.
[b] Mean ± SEM of n = 2 independent experiments.
[c] Unable to generate IC_{50} value at the tested concentration range.

positive hit as a compound that exhibits ≥40% mean percent inhibition. By applying this cut-off value, 13 compounds were identified as potential MRP1 inhibitors. These are displayed as green dots in the 3D plot. Identified MRP1 hits, together with their therapeutic targets and percent inhibition are shown in Table 1. Among the identified compounds, cyclosporine A and rapamycin are known MRP1 inhibitors [35,36], while the others, to the best of our knowledge, have not been reported to inhibit MRP1 efflux function. The reproducibility of the screening assay was reflected by the correlations between any two experiments, which are in the range of 0.86–0.94, indicating a good reproducibility. The performance of the assay was also assessed by deriving the Z'-factor from the experiments. The average Z'-factor across all plates was 0.63, indicating a good assay performance.

3.3. Validation of identified MRP1 inhibitors

To verify the inhibitory activities of the hit compounds obtained from the initial high-content screening and to identify any false hits or auto fluorescent compounds, we performed concentration-response studies using the same high-content imaging-based calcein efflux assay with compound concentrations ranging from 0.4 to 50 μM. One of the compounds, deltarasin, was excluded from further studies as we did not observe concentration-dependent inhibition of calcein efflux, possibly due to its cytotoxic effect (data not shown). We were also unable to obtain a sigmoidal concentration response curve and the corresponding IC_{50} value for the compound CX-6258, due to a cytotoxic effect at higher concentrations. Chemical structures of the positive hits are shown in Fig. 4. As shown in Fig. 5, 11 of the identified MRP1 inhibitors exhibit sigmoidal concentration-dependent inhibition of calcein efflux. JNJ-26854165, a compound that did not inhibit MRP1 in the initial screen was also included as a negative control and exhibited no modulatory effect on calcein efflux at the tested concentration range. As detailed in Table 1, IC_{50} values in the low micromolar range of 0.7–8.5 μM were displayed by the tested compounds, which are comparable to MK571 (IC_{50} = 8.4 ± 1.8 μM). Next, we examined if the MRP1-inhibitory activity of the identified compounds can be reproduced in the traditional flow cytometry-based calcein accumulation assay. To this end, H69 and H69AR cells were pre-treated with the test compounds for 10 min before incubation with calcein for 30 min. As shown in Fig. 6A, MK571 at 50 μM enhanced calcein accumulation in H69AR cells by 12.7-fold. All of the identified compounds (10 μM) also significantly increased calcein accumulation in H69AR cells by 6.6–13.0-fold, but not in H69 cells. Test compounds AZD1208, YM201636, and everolimus were the most potent calcein efflux inhibitors and increased calcein accumulation by 13.0-, 10.5-, and 10.8-fold, respectively. In contrast, JNJ-26854165, which was used as a negative control, did not result in an appreciable change of calcein accumulation in both cell lines.

To investigate if the identified MRP1 inhibitors modulate the efflux of other MRP1 substrates besides calcein, we studied the effects of the compounds on MRP1-mediated efflux of a commonly used anticancer drug, doxorubicin, a well-known substrate of MRP1. HEK293T cells were transiently transfected with MRP1-GFP encoding vector and confocal microscopy was used to visualize the inhibitory effect of the test compounds on MRP1-mediated doxorubicin efflux in live cells. As shown in Fig. 6B, cells treated with DMSO showed high doxorubicin accumulation in the nuclei of non-transfected cells, while doxorubicin fluorescence was very low or undetectable in cells expressing MRP1-GFP. MRP1-mediated efflux of doxorubicin was reduced by MK571 (50 μM) but not

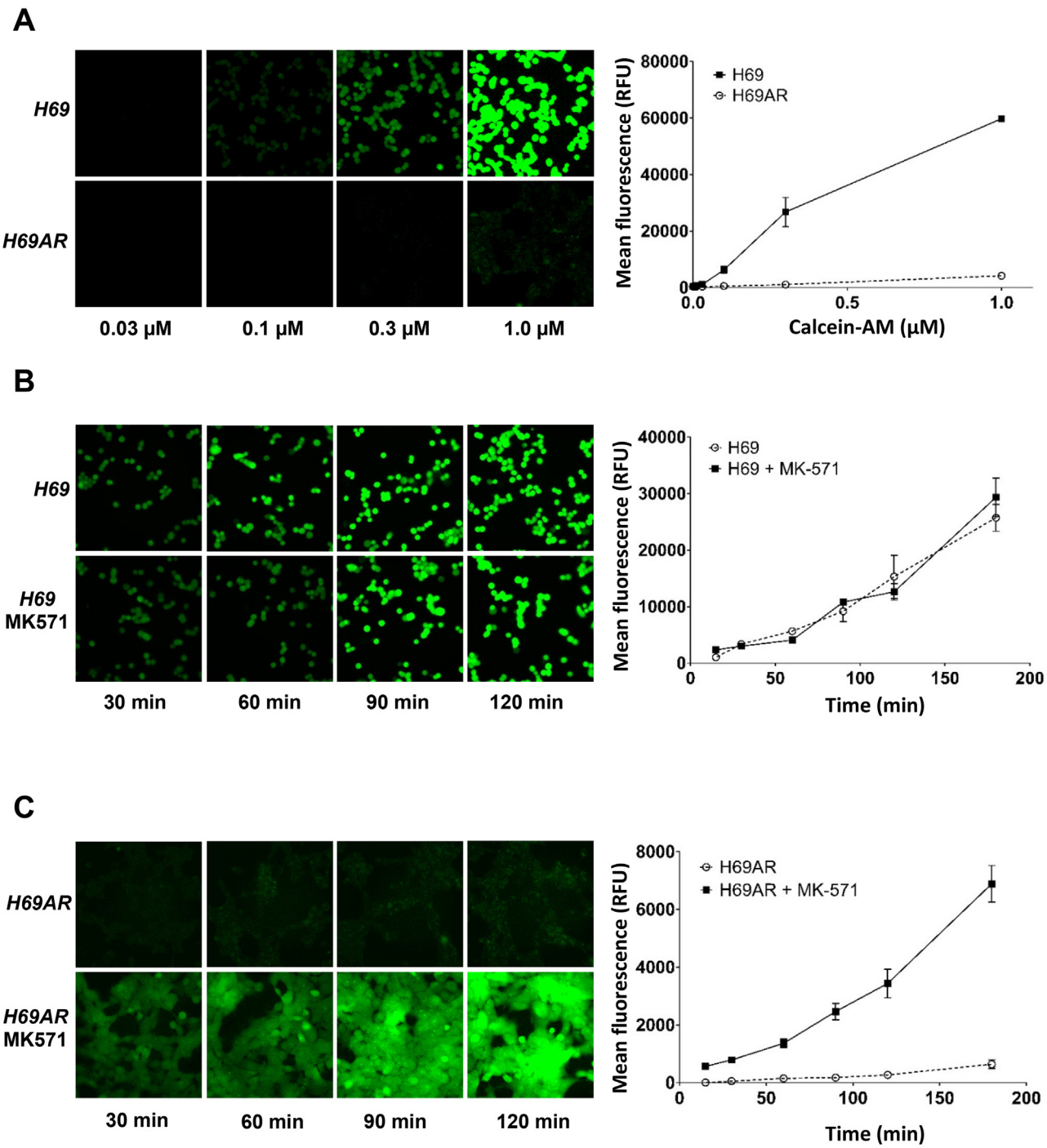

Fig. 2. Concentration- and time-dependent accumulation of calcein in H69 and H69AR cells. A. H69 and H69AR cells were treated with calcein-AM at various concentrations (0.001–1 μM) for 1 h. Representative images of calcein-AM treatment at 0.03, 0.1, 0.3, and 1 μM are shown. The average fluorescence intensities derived from the fluorescent images were graphed and shown on the right. B. H69 cells were treated with 0.25 μM calcein-AM in the absence and presence of 50 μM MK571 for 15–180 min. Representative images of calcein treatment at 30, 60, 90, and 120 min are shown. C. H69AR cells were treated with 0.25 μM calcein-AM in the absence and presence of 50 μM MK571 for 15–180 min. Representative images of calcein treatment at 30, 60, 90, and 120 min are shown. Data are representative of two experiments and shown as mean ± SD (n = 3).

JNJ-26854165 (10 μM), which were used as positive and negative controls, respectively. All the test compounds (10 μM) appear to induce doxorubicin accumulation in MRP1-expressing cells to a certain extent, with tipifarnib, AZD1208, deforolimus, HS-173, and YM201636 showing strong inhibition, while rapamycin, ESI-09, everolimus, TAK-733, CX-6258, cyclosporine A, and temsirolimus showing moderate to mild inhibition.

3.4. Resistance reversal by selected MRP1 inhibitors

The anti-cancer agent library used in this study contains small molecules currently under clinical investigation for different therapeutic targets, such as mTOR and PI3K. We were interested to investigate if the identified MRP1 inhibitors can reverse drug resistance in an MDR cell line. Such property may be valuable in treatment of cancers with prominent MRP1 expression. We first performed concentration response using the identified compounds

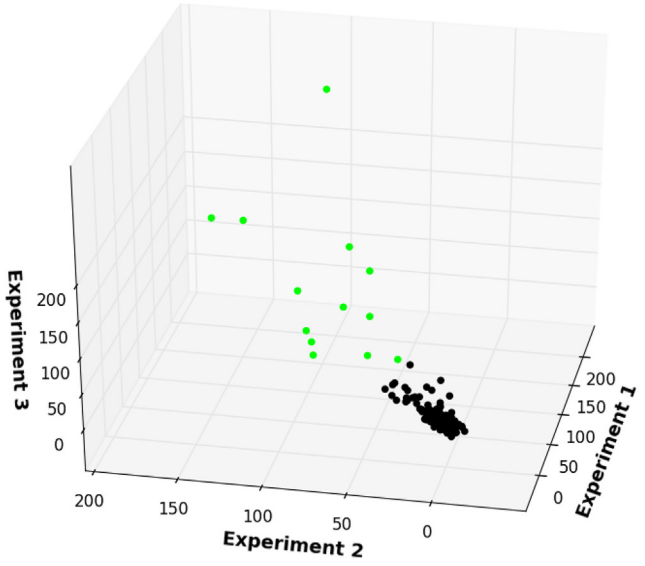

Correlation coefficient

Experiment	1	2	3
1	1.00		
2	0.89	1.00	
3	0.94	0.86	1.00

Fig. 3. Reproducibility of the imaging-based MRP1-mediated calcein accumulation screening assay. Screening of the anti-cancer compound library was performed in three independent experiments at compound concentration of 10 μM. The relative inhibitory activities of each compound were calculated and displayed as a 3D plot. Green dots represent compounds with mean percent inhibition of ≥40%. The table below the plot shows correlation coefficients between any two experiments. 3D scatter plot was generated using Matplotlib 1.5.1 and correlation coefficients were calculated using MS Excel.

in H69AR to evaluate the cytotoxicity of the compounds (data not shown). Selected compounds at non- or minimal cytotoxic concentrations were then administered to H69AR cells in combination with increasing concentrations of vincristine, a commonly used chemotherapeutic agent. As shown in Fig. 7, H69 cells (dotted blue) exhibited a much greater sensitivity towards vincristine than H69AR cells (solid red). MK571, tipifarnib, AZD1208, rapamycin, deforolimus, everolimus, TAK-733, and temsirolimus at indicated concentrations reversed the resistance of H69AR cells against vincristine to various extents. IC_{50} values and fold resistance of H69AR cells treated with vincristine with or without the selected compounds are shown in Table 2. In the absence of any MRP1 inhibitor, H69AR cells were 43.6-fold more resistant than the parental H69 cells against vincristine. The standard MRP1 inhibitor MK571 at 10 μM reduced the resistance of H69AR cells to 19.4-fold. Comparably, tipifarnib, AZD1208, deforolimus, and temsirolimus reversed the resistance of H69AR cells against vincristine to 11.6–22.1-fold. On the other hand, rapamycin, everolimus, and TAK-733 resulted in stronger reduction in fold resistance (≤10-fold). These data indicate that the identified MRP1 inhibitors may be potent MDR reversal agents, which can be studied for their effectiveness in overcoming clinical MDR where MRP1 expression is directly linked to a poor clinical outcome.

Table 2
The effects of selected MRP1 inhibitors on the IC_{50} values of vincristine in H69 and H69AR cells.

Cells/Treatment	IC_{50}[a] (nM)	Fold resistance[b]
H69	0.5 ± 0.2	1.0
H69AR	23.1 ± 3.0	45.5
H69AR + MK571 10 μM	9.8 ± 0.4	19.4
H69AR + Tipifarnib 1 μM	6.4 ± 0.3	12.7
H69AR + AZD1208 2 μM	11.4 ± 0.7	22.6
H69AR + Rapamycin 10 μM	4.0 ± 0.9	7.8
H69AR + Deforolimus 10 μ	8.7 ± 1.1	17.1
H69AR + Everolimus 10 μM	6.6 ± 1.9	13.1
H69AR + TAK-733 10 μM	5.5 ± 0.5	10.8
H69AR + Temsirolimus 10 μM	9.0 ± 0.6	17.7

[a] Mean ± SEM of n ≥ 3 independent experiments.
[b] Fold resistance is the ratio between IC_{50} value of each treatment and IC_{50} value of vincristine alone in H69 cells (0.5 ± 0.2).

3.5. Differential effects of hit compounds on $E_2$17βG vesicular uptake by MRP1-4

Several other members of the MRP (ABCC) sub-family, like MRP1, hold important roles in regulating drug absorption and disposition in different organs [11]. We were interested to investigate whether the MRP1 inhibitors identified in our study also exert a modulatory activity on other MRPs and learn about their selectivity towards closely related sub-family members. To this end, we prepared membrane vesicles from HEK293 cells stably or transiently expressing MRP1-4 and evaluated the effects of the compounds on the uptake of $E_2$17βG, a common MRP substrate, into the membrane vesicles. As shown in Fig. 8, uptake of [^{3}H]$E_2$17βG into MRP1-4 membrane vesicles was reduced by more than 50% with 10 μM MK571, a pan-MRP inhibitor. Another known broad-spectrum MRP inhibitor, cyclosporine A, also displayed significant inhibition of [^{3}H]$E_2$17βG uptake across MRP1-4 membrane vesicles. In addition, the mTOR inhibitors, rapamycin and its derivatives deforolimus, everolimus, and temsirolimus appear to be pan-inhibitors for MRP1-4, effectively reducing [^{3}H]$E_2$17βG uptake across MRP1-4 membrane vesicles. In terms of compound effects on MRP1-mediated transport of $E_2$17βG, all of the hit compounds except TAK-733 resulted in a significant decrease in the uptake of [^{3}H]$E_2$17βG into MRP1 membrane vesicles. Tipifarnib, rapamycin, deforolimus, ESI-09, everolimus, CX-6258, and temsirolimus inhibited [^{3}H]$E_2$17βG uptake by more than 50%, while AZD1208 and YM201636 showed inhibitory activity in the range of 20–50%. ESI-09 was the most potent inhibitor of [^{3}H]$E_2$17βG uptake by MRP1, reducing the update by 90%. Interestingly, two of the hit compounds, namely tipifarnib and ESI-09, resulted in 2.2- and 2.1-fold stimulation of [^{3}H]$E_2$17βG uptake, respectively, into MRP2 membrane vesicles. HS-173, YM201636, and CX-6258 also displayed a mild stimulatory effects of 17, 29, and 16%, respectively on MRP2-mediated transport, although the results are not statistically significant. In MRP3 membrane vesicles, tipifarnib is the only compound apart from cyclosporine A and rapamycin and its derivatives that exerted a significant inhibitory effect on [^{3}H]$E_2$17βG uptake. In contrast, all of the test compounds exhibited a significant inhibitory activity on [^{3}H]$E_2$17βG uptake into MRP4 membrane vesicles.

3.6. Identified hit compounds directly interact with MRP1

We recently introduced a novel structural-based approach for the screening of drug libraries for interactions with ABC transporters by genetically engineering a two-color MRP1 protein that is capable of detecting direct interaction of drug molecules with MRP1. This approach is based on fusing a GFP and RFP with MRP1 to yield a modified two-color recombinant protein, which reports changes in intramolecular FRET efficiency as an index of MRP1 con-

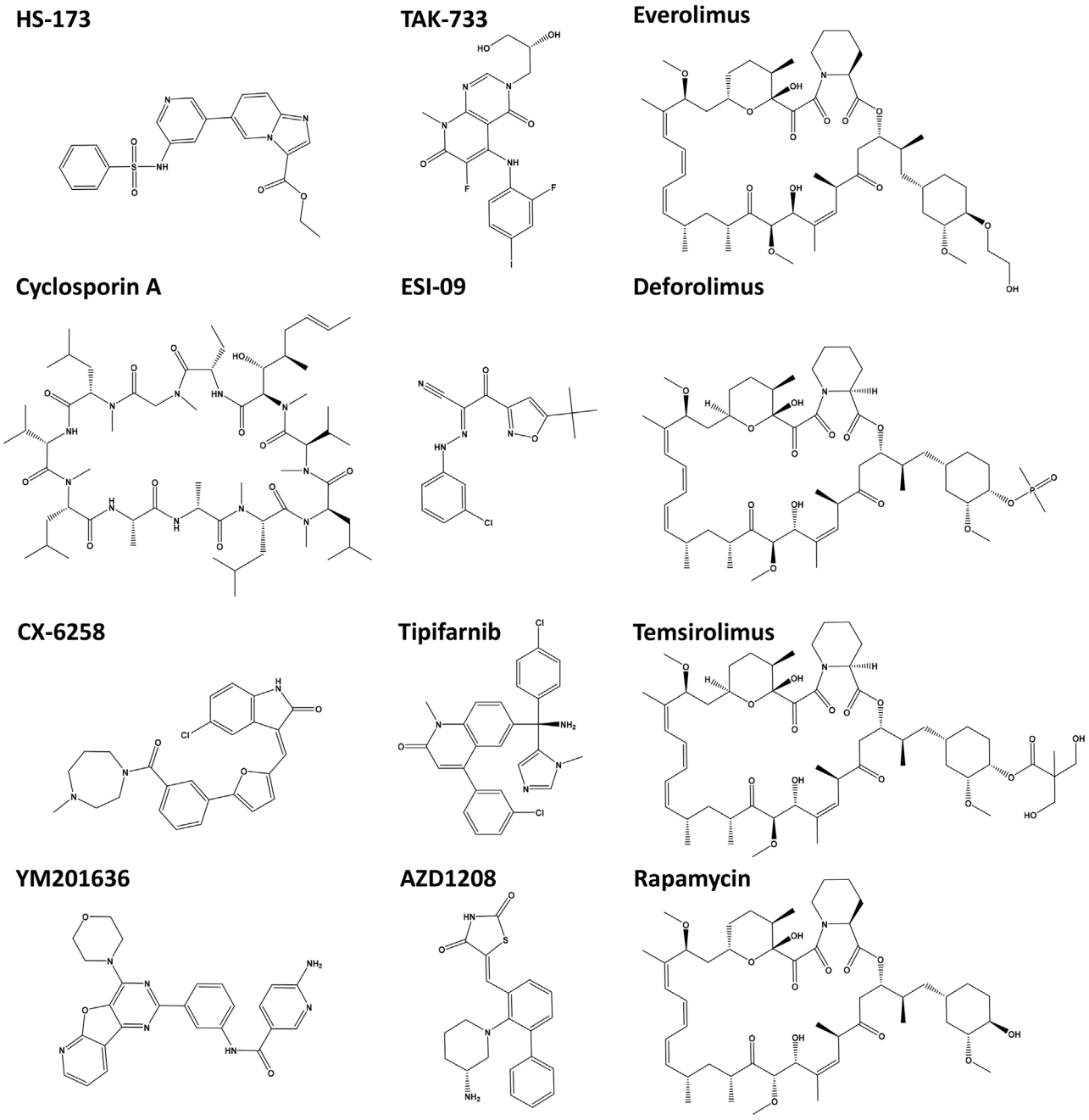

Fig. 4. Chemical Structures of selected compounds.

formational changes upon ligand binding [58]. In the present study, we used fluorescence spectroscopy approach to determine changes in FRET efficiency of the two-color MRP1 protein upon interaction with the hit compounds. Our results indicate that MK571, a known MRP1 inhibitor, produced ~8% increase in FRET efficiency relative to the apo condition (Fig. 9). Similarly, all of 12 test compounds caused an increase in FRET efficiency relative to the basal FRET level of the apo protein reflecting direct interaction with MPR1. In contrast, JNJ-26854165, which did not induce MRP1 inhibition in functional assays also did not produce any significant FRET change relative to the apo FRET levels. Among the hit compounds, tipifarnib showed the smallest FRET change (~2.5%) and deforolimus induced the largest FRET change (~9%).

4. Discussion

MRP1 predominantly localizes at the basolateral membranes of epithelial cells and plays an important role in regulating the absorption and distribution of various xenobiotics, including many therapeutic agents and toxins. For tissues with epithelial basolateral membranes confronting the blood circulation, MRP1 limits the entry of blood-borne xenobiotics and thus lower their bioavailability or potential toxic effects. For instance, Mrp1 knockout mice show greater sensitivity towards damages of the oropharyngeal mucosal layer and the testicular tubules induced by etoposide, an anti-cancer agent [37]. Therefore, profiling the interactions between therapeutic agents and MRP1 represents an important aspect in predicting and determining drug bioavailability and drug–drug interactions mediated by MRP1. In addition, MRP1

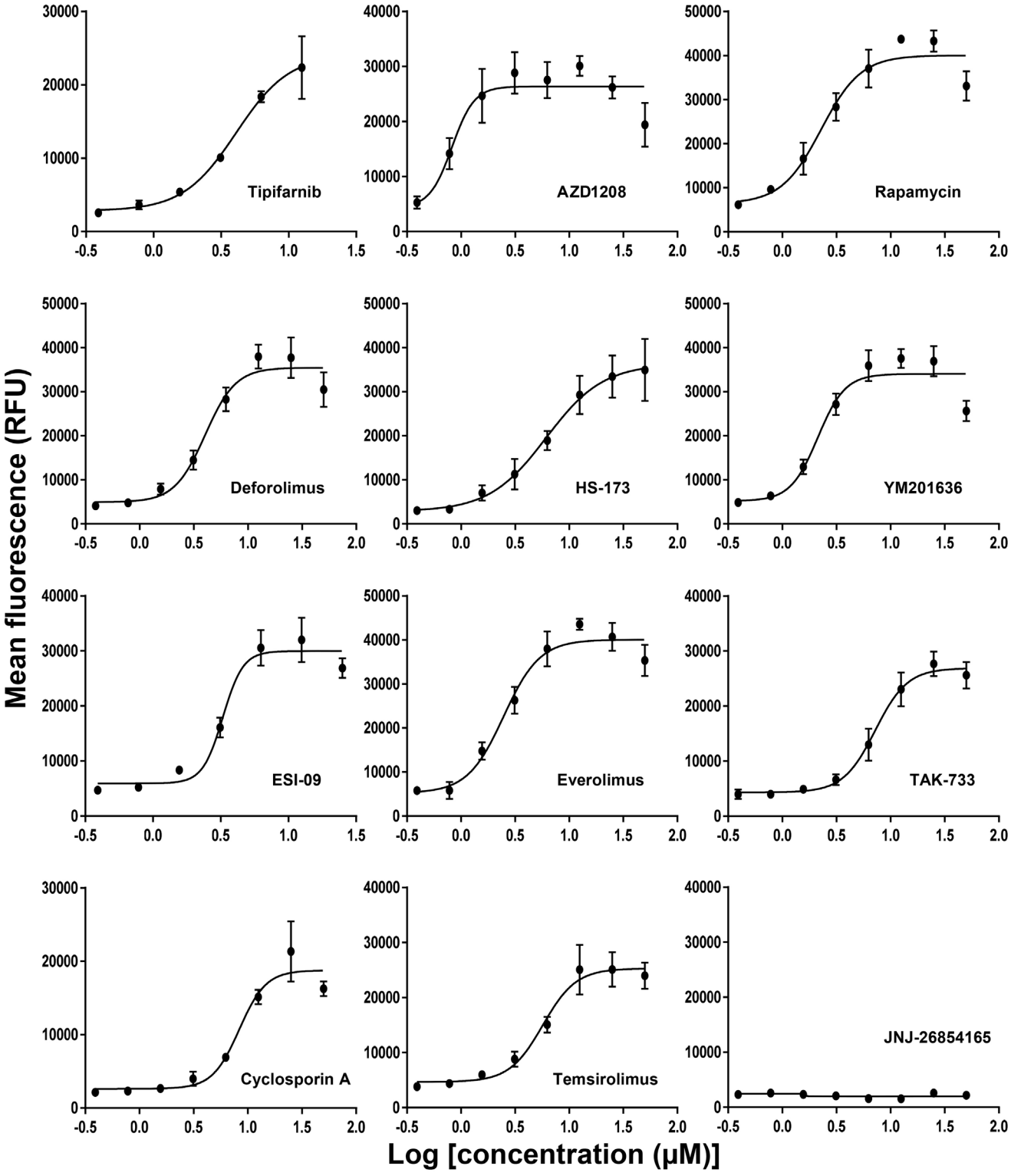

Fig. 5. Concentration response curves of positive hits identified from initial screening. H69AR cells were pre-treated with indicated compounds at concentrations from 0.4 to 50 μM for 30 min before treatment with 0.25 μM calcein-AM for 1 h. One of the identified compounds, deltarasin, did not exhibit concentration-dependent inhibition (data not shown) and was excluded from further studies. JNJ-26854165 was not an initial positive hit and included as a negative control.

is associated with clinical MDR of several types of cancers. Re-sensitization of resistant malignancies using MRP1 inhibitors remains a possible avenue in overcoming MDR in chemotherapy, especially in cancers where MRP1 expression is clearly associated with a poor clinical outcome.

In this study, we have developed and validated a high content imaging-based high-throughput assay for the detection of MRP1 inhibition via calcein efflux in an MRP1-overexpressing cell line and performed screening of an anti-cancer agent library using this assay. Based on three independent screenings, the assay demonstrated very high correlation (0.86–0.94) among replicates. The

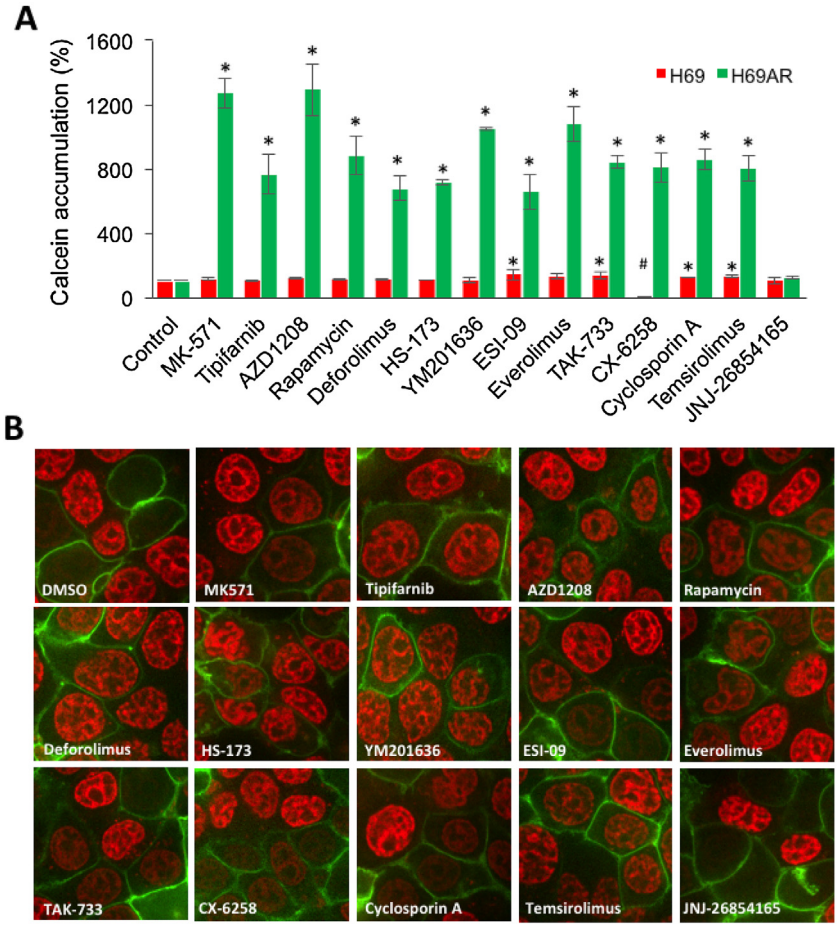

Fig. 6. Validation of MRP1-inhibitory activity of identified compounds. A. H69 and H69AR cells were pre-treated with 50 μM MK571 or 10 μM test compounds for 10 min before treatment with 25 nM calcein-AM at 37 °C for 30 min. Fluorescence intensities of intracellular calcein were detected using flow cytometry, with excitation and emission wavelengths of 480 and 533/30 nm, respectively. Data are combined from two experiments and presented as mean ± SEM. *, $p < 0.05$ compared with control; #, excluded due to significant change in cell scatter. B. HEK293T cells transiently transfected with MRP1-GFP (green) were pre-treated with 10 μM test compounds, before treatment with doxorubicin (red) at 37 °C for 1 h. Images were acquired using confocal microscopy. GFP and doxorubicin were excited at 488 nm, and detected at 475/42 and 605/64 nm, respectively.

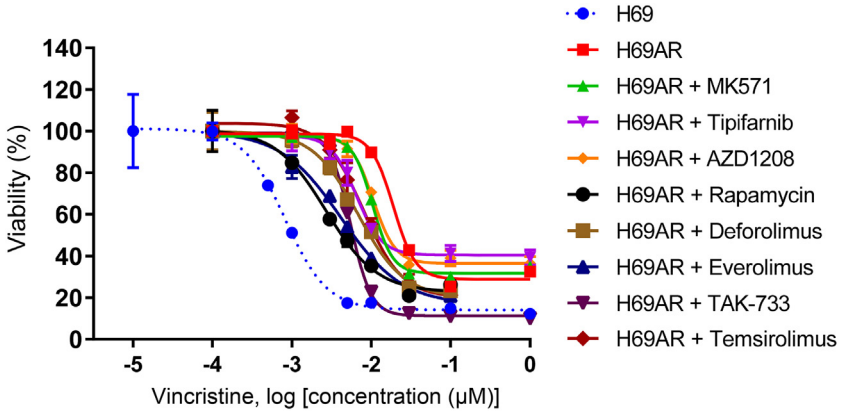

Fig. 7. Reversal of drug resistance towards vincristine in H69AR cells by selected identified MRP1 inhibitors. H69 and H69AR cells were treated with vincristine at increasing concentrations in the absence and/or presence of selected MRP1 inhibitors. MK571, rapamycin, deforolimus, everolimus, TAK-733, and temsirolimus were at 10 μM. Tipifarnib and AZD1208 were at 1 and 2 μM, respectively. After 72 h, cell viability was evaluated with MTT. Data are representative of two experiments and presented as mean ± SD (n = 3).

high quality and efficiency of this high-throughput screening assay was also reflected by Z'-factor of 0.63 (across all plates). The imaging-based efflux assay described in this study has several advantages over assays based on fluorescent plate readers and flow cytometry. In terms of sensitivity, the imaging-based assay is superior to assays based on fluorescent plate reader, which is more suited for assays performed in a homogenous condition [30]. Additionally, unlike assays based on flow cytometry, cells can be imaged *in situ* without the need of preparing cell suspension and performing multiple washing steps, which increase the processing time and

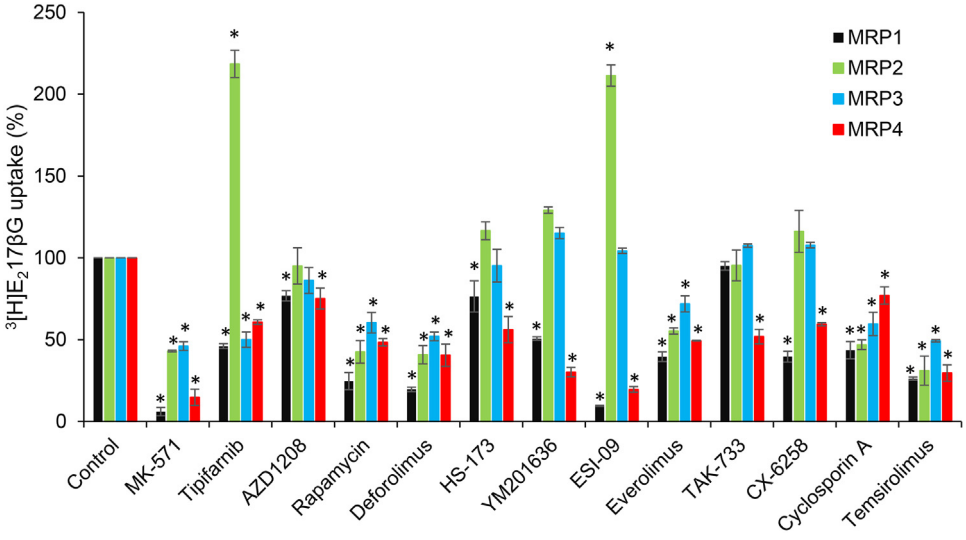

Fig. 8. Effects of test compounds on [^{3}H]$E_2$17βG uptake into MRP1, 2, 3, and 4 membrane vesicles. Membrane vesicles were prepared from stable HEK293/MRP1 and HEK293/MRP3 cells or transiently transfected HEK293T/MRP2 and HEK293T/MRP4 cells. Membrane vesicles (2 μg protein) were incubated with 10 μM test compounds. For vesicular transport into MRP1 membrane vesicles, reactions were performed using 400 nM/20 nCi [^{3}H]$E_2$17βG at 37 °C for 1 min. For studies using MRP2-5 membrane vesicles, reactions were performed using 400 nM/50 nCi [^{3}H]$E_2$17βG at 37 °C for 5 min. Radioactivity retained on collected membrane vesicles was quantified using liquid scintillation counting. Data are combined from two experiments and presented as mean ± SEM. *, $p < 0.05$ compared with control.

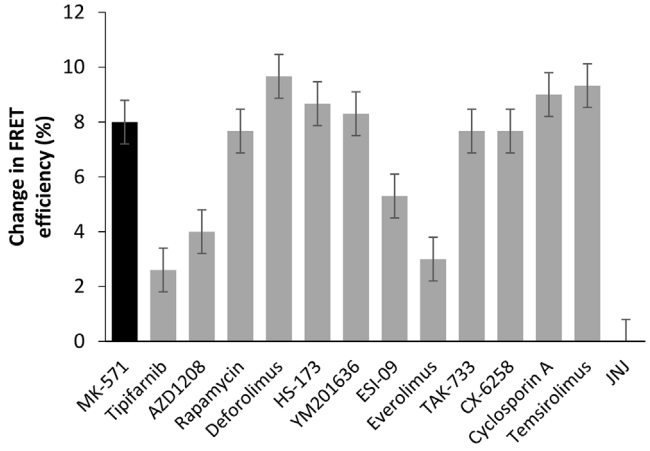

Fig. 9. Compound induced conformational changes in MRP1. Membrane vesicles were prepared from stable HEK293/GFP-MRP1 and HEK293/two-color MRP1 cells. Membrane vesicles (10 μg) were incubated with 10 μM of each test compound for 20 min at 37 °C prior fluorescence spectroscopy using Fluorimeter model FL3-11. GFP excitation was accomplished at 480 nm and RFP was excited at 530 nm. Emission for both GFP and RFP with integration time of 3 s was recorded at 480–650 nm. GFP excitation was observed at 480 nm and RFP, at 530 nm. Emission for both GFP and RFP was collected at 480–650 nm with 3-s integration time. Data are representative of two independent experiments in triplicates. MK571 and JNJ-26854165 were used as positive and negative controls, respectively. To calculate the change in FRET efficiency for test compound conditions, the basal apo FTRET efficiency was subtracted from the compound-induced FRET efficiencies and results are presented as mean ± SEM.

limit the assay throughput. Furthermore, cell viability and density before and after treatment can be visually inspected in bright-field images. This assists in the evaluation of compound cytotoxicity, which may interfere with the assay. In this report, although we collected both bright-field and fluorescent images from the experiments, the automated image analysis requires only the fluorescent images for the generation of segmentation masks. The processing time for image acquisition can be considerably reduced if bright-field images are not collected. This may be desirable for compound screening at a much larger scale or for conservation of data storage space. A caveat associated with our assay, however, is a gradual decrease in fluorescence levels as the plate is read. We think that efflux of calcein out of the cells after the treatment removal and washing step is causing a time-dependent reduction in intracellular calcein levels. Therefore, it is crucial to have controls placed throughout the plate to account for the fluorescence decrease. In our screening, one positive and one negative controls were included in every two columns so the percent inhibition for each test compound was calculated on a two column basis. It is also possible to circumvent this issue by reducing the plate reading time by decreasing the number of images acquired.

Conventional cytotoxic drugs such as doxorubicin, etoposide, paclitaxel, cisplatin, and methotrexate, which are still commonly used in chemotherapy, target essential and fundamental cellular processes (e.g., DNA synthesis, cell division, or DNA damage) that makes them non-selective and cytotoxic. Major problems associated with chemotherapy are the development of MDR and toxicity. One way to address these problems is the focus on discovering new drugs that target cell signaling pathways and are not cytotoxic. Several new agents have been discovered that target different kinases and receptors (e.g. drugs that target tyrosine kinases and EGF receptor). Another common strategy to improve the efficacy and reduce the toxicity of chemotherapeutic drugs is through combination therapy, where drugs from different families targeting different mechanisms are administered together to achieve better outcomes. Given the remarkable ability of MRP1 to modulate the absorption and distribution of a wide spectrum of drugs, it is very important to profile any new drug candidates for their interaction with this transporter. In the present work, we tested the interactions between MRP1 and anti-cancer agents that are currently under clinical investigation. We are particularly interested in anti-cancer candidates, as a positive inhibitory activity on MRP1 not only suggests a potential application in reversing MRP1-mediated drug resistance, but may also indicate a substrate relationship with MRP1. In the former scenario, the drug candidate may be used as an anti-cancer agent that can also reverse MRP1-mediated drug resistance. In the latter scenario, the anti-cancer agent might eventually become ineffective due to MDR conferred by MRP1 overexpression. Information on such interactions thus provide insights into the possible interactions and efficacy of the drugs. In terms of MDR reversal in the clinical setting, although no clinical trial aimed at MRP1

inhibition has been reported, clinical trials using P-gp inhibitors as chemosensitizers have continued to produce negative results [38]. In unraveling the failure of translating preclinical and early clinical successes of P-gp inhibitors into phase III clinical trials, a few possible explanations have been put forward, notably the lack of selection of patient population (in which upregulated P-gp expression in patients is confirmed) and the possible compensatory increase in drug efflux by other ABC transporters [39]. Therefore, the potential application of MRP1 inhibitor in sensitizing malignancies where MRP1 expression is prominent, such as primary neuroblastoma, to chemotherapeutic agents cannot be ruled out. A combinatorial approach targeting multiple MDR transporter, such as P-gp, MRP1, and BCRP, may also yield a more fruitful outcome if multiple drug transporters indeed work concertedly in modulating drug efflux in cancer cells.

Among the 12hit compounds identified in the current study, cyclosporine A and rapamycin have been previously shown to inhibit the efflux function of MRP1 [35,36]. Cyclosporin A and rapamycin are also known to inhibit the transport function of other ABC drug transporters, including P-gp, BCRP, and MRP2 [36,40]. Three of the novel inhibitors identified in this study, namely deforolimus, everolimus, and temsirolimus are first-generation rapamycin analogs (rapalogs) [41]. Rapamycin and rapalogs are inhibitors of mTOR (mammalian target of rapamycin), an intracellular serine/threonine kinase functioning downstream of the phosphoinositide 3-kinase (PI3K)/Akt signaling pathway. mTOR holds essential roles in regulating cell growth, proliferation, and survival and is dysregulated in various cancers [42]. The use of rapalogs has shown promising clinical efficacy in several types of cancers and numerous ongoing clinical trials are using rapalogs as a single agent or in combination with other anti-cancer agents in treatments for a wide range of cancers [43,44]. In the present study, we demonstrated that deforolimus, everolimus, and temsirolimus are pan-inhibitors of MRP1-4. These rapalogs have also been shown to be inhibitors of P-gp [33]. Therefore, like cyclosporine A, they are likely to be broad-spectrum inhibitors of ABC drug transporters. Whether these rapalogs exert the inhibitory activity by competitive binding and are thus substrates of ABC drug transporters remains to be elucidated. If the rapalogs are indeed substrates of ABC drug transporters, they will be at risk for multidrug resistance interference mediated by these transporters. In addition, everolimus has also been reported to downregulate the expression levels of MRP1 in a cisplastin-resistant gastric cancer cell line [45]. It is possible that the downregulation by everolimus is achieved by the disruption of the PI3K/Akt pathway, which has been demonstrated to modulate the expression of MRP1 in human acute myelogenous leukemia [46]. It is interesting to note that among the tested compounds, rapamycin was the most successful in reversal of H69AR cells resistance towards anti-cancer drug vincristine (IC_{50} value decreased from 23.1 to 4.0 nM). Everolimus, deforolimus, and temsirolimus also decreased resistance of H69AR cells against vincristine to IC_{50} values of 6.6, 8.7, and 9 nM, respectively.

Among the identified novel MRP1 inhibitors, HS-173 and YM201636 are potent PI3K inhibitors that are being actively investigated for their anti-cancer efficacy [47,48]. It will be of interest to investigate if these PI3K inhibitors modulate the expression level of MRP1, besides inhibiting its transport function. The observation that certain small molecules can modulate not only the efflux activity but also the expression or degradation of ABC drug transporters has led to the possibility of sensitizing ABC transporter-mediated MDR by exploiting these alternative mechanisms. For instance, PZ-39 and several related compounds have been reported to effectively induce the endocytosis and trafficking of BCRP to lysosomes for degradation, in addition to inhibiting its transport function [49]. The effectiveness of such dual-mode inhibitor of ABC transporters in clinical chemotherapy is yet to be verified but certainly worth exploring. Two of the identified MRP1 inhibitors, AZD1208 and CX-6258 are potent pan-Pim kinase inhibitors and have shown promising preclinical chemotherapeutic efficacy [50,51]. Interestingly, the Pim-1 kinase has been reported to interact with and promote the functions of P-gp and BCRP. Phosphorylation of BCRP by Pim-1 kinase accommodates the multimerization of BCRP in a prostate cancer cell line whereas phosphorylation of P-gp by Pim-1 enables glycosylation and surface expression of P-gp besides protecting it from proteasomal degradation [52,53]. In both cases, inhibition of Pim-1 kinase either by gene knockdown or chemical inhibitor resensitizes resistant cells to chemotherapeutic agents [52,53]. Hence, it will be of interest to investigate if Pim kinase modulates the expression and degradation of MRP1, and if inhibition of Pim kinase by AZD1208 and CX-6258 can abolish MRP1-mediated MDR through these mechanisms.

In order to investigate the effects of the identified hit compounds on closely related MRP family members, vesicular transport studies were conducted by measuring the uptake of [^{3}H]$E_2$17βG by MRP1-4. Our results indicate some selectivity towards the target transporters as well as differential modulation of transport activity by the hit compounds. For instance, while most of the compounds exhibited an inhibitory effect, tipifarnib and ESI-09 notably potentiated the uptake of [^{3}H]$E_2$17βG by MRP2. Stimulation of MRP2-mediated uptake has been previously reported in other studies. For instance, a panel of drugs including indomethacin, probenecid, sulfinpyrazone, and sulfanitran strongly stimulate the uptake of $E_2$17βG in MRP2-overexpressing Sf9 membrane vesicles, while the efflux of anti-cancer agents paclitaxel and docetaxel by MRP2 in the polarized MDCKII (Madin-Darby canine kidney) cells is substantially stimulated by probenecid [54,55]. As MRP2 is a drug efflux transporter with clinical importance [56], stimulation of MRP2 by tipifarnib and ESI-09 could give rise to clinically relevant drug–drug interactions where the bioavailability of a co-administered MRP2 substrate drug could be unfavorably decreased. However, it should be noted that whether a test compound stimulates or inhibits MRP2 in the vesicular transport assay can be probe-dependent. Such complexity in MRP2-mediated transport is highlighted in a study by Kidron et al., in which five out of eight test compounds exhibit different effects (stimulatory, inhibitory, or ineffective) on MRP2-mediated transport depending on whether LTC_4, $E_2$17βG, or 5(6)-carboxy-2,7-dichlorofluorescein is used as the probe substrate [57]. Therefore, further interpretation and studies on the effects of tipifarnib and ESI-09 on MRP2 will need to take into account the possible probe-dependent differences. In addition, it is noteworthy that HS-173, YM201636 (PI3K inhibitors) and AZD1208, CX-6258 (pan-Pim kinase inhibitors) showed inhibition of $E_2$17βG transport by MRP1 and MRP4 but not by MRP2 and MRP3.

In summary, we demonstrated the effectiveness of the high content imaging-based MRP1-inhibition assay to study compound interaction with MRP1. This paves the way for further screening methods for the high throughput functional studies of MRP1, such as compound effect on MRP1 expression and trafficking using the imaging-based system. We also identified novel inhibitors of MRP1 and demonstrated their ability to reverse drug resistance in MRP1-overexpressing cells. Anti-cancer agents that show a lack of interaction with MRP1 in our study might also be at lower risk of being interfered by MRP1-mediated MDR.

Conflict of interest

The authors declare no conflict of interest.

Acknowledgements

This work was supported by Research/Scholarship Support Fund (SDSU), Scholarly Excellence Funds (SDSU), and Lab Start-up funds

to Surtaj H. Iram. We thank Dr. Suresh V. Ambudkar (NIH, MD), Dr. Alfred Schinkel, Prof. Piet Borst (The Netherlands Cancer Institute, the Netherlands), and Dr. Adam Hoppe (South Dakota State University, SD) for providing the cell lines used in this study. We also thank Dr. Adam Hoppe and members of his laboratory for assistance with confocal microscope and flow cytometer. Surtaj H. Iram is a member of BioSNTR.

References

[1] M. Dean, T. Annilo, Evolution of the ATP-binding cassette (ABC) transporter superfamily in vertebrates, Annu. Rev. Genomics Hum. Genet. 6 (2005) 123–142.
[2] M. Dean, R. Allikmets, Complete characterization of the human ABC gene family, J. Bioenerg. Biomembr. 33 (2001) 475–479.
[3] Y. Li, J. Revalde, J.W. Paxton, The effects of dietary and herbal phytochemicals on drug transporters, Adv. Drug Deliv. Rev. (2016), http://dx.doi.org/10.1016/j.addr.2016.09.004, September. pii: S0169-409X(16)30259-9. [Epub ahead of print].
[4] G. Szakacs, A. Varadi, C. Ozvegy-Laczka, B. Sarkadi, The role of ABC transporters in drug absorption, distribution, metabolism, excretion and toxicity (ADME-Tox), Drug Discov. Today 13 (2008) 379–393.
[5] S.H. Iram, S.P.C. Cole, Mutation of Glu521 or Glu535 in cytoplasmic loop 5 causes differential misfolding in multiple domains of multidrug and organic anion transporter MRP1 (ABCC1), J. Biol. Chem. 287 (March (10)) (2012) 7543–7555.
[6] M. Dean, Y. Hamon, G. Chimini, The human ATP-binding cassette (ABC) transporter superfamily, J. Lipid Res. 42 (2001) 1007–1017.
[7] K. Moitra, M. Dean, Evolution of ABC transporters by gene duplication and their role in human disease, Biol. Chem. 392 (2011) 29–37.
[8] Guidance for Industry (Draft): Drug Interaction Studies – Study Design, Data Analysis, Implications for Dosing, and Labeling Recommendations. http://wwwfdagov/downloads/drugs/guidancecomplianceregulatoryinformation/guidances/ucm292362pdf. Accessed 27 September 2016.
[9] S.P. Cole, G. Bhardwaj, J.H. Gerlach, J.E. Mackie, C.E. Grant, K.C. Almquist, et al., Overexpression of a transporter gene in a multidrug-resistant human lung cancer cell line, Science 258 (1992) 1650–1654.
[10] M.J. Flens, G.J. Zaman, P. van der Valk, M.A. Izquierdo, A.B. Schroeijers, G.L. Scheffer, et al., Tissue distribution of the multidrug resistance protein, Am. J. Pathol. 148 (1996) 1237–1247.
[11] A.H. Schinkel, J.W. Jonker, Mammalian drug efflux transporters of the ATP binding cassette (ABC) family: an overview, Adv Drug Deliver Rev. 64 (2012) 138–153.
[12] S.H. Iram, S.P.C. Cole, Expression and function of human MRP1 (ABCC1) is dependent on amino acids in cytoplasmic loop 5 and its interface with nucleotide binding domain 2, J. Biol. Chem. 286 (9) (2011).
[13] G. Jedlitschky, I. Leier, U. Buchholz, K. Barnouin, G. Kurz, D. Keppler, Transport of glutathione, glucuronate, and sulfate conjugates by the MRP gene-encoded conjugate export pump, Cancer Res. 56 (1996) 988–994.
[14] R. Beedholm-Ebsen, K. van de Wetering, T. Hardlei, E. Nexo, P. Borst, S.K. Moestrup, Identification of multidrug resistance protein 1 (MRP1/ABCC1) as a molecular gate for cellular export of cobalamin, Blood 115 (2010) 1632–1639.
[15] A.J. Slot, S.V. Molinski, S.P. Cole, Mammalian multidrug-resistance proteins (MRPs), Essays Biochem. 50 (2011) 179–207.
[16] S.P. Cole, Targeting multidrug resistance protein 1 (MRP1, ABCC1): past, present, and future, Annu. Rev. Pharmacol. Toxicol. 54 (2014) 95–117.
[17] M.M. Gottesman, O. Lavi, M.D. Hall, J.P. Gillet, Toward a better understanding of the complexity of cancer drug resistance, Annu. Rev. Pharmacol. Toxicol. 56 (2016) 85–102.
[18] H. Burger, K. Nooter, G.J. Zaman, P. Sonneveld, K.E. van Wingerden, R.G. Oostrum, et al., Expression of the multidrug resistance-associated protein (MRP) in acute and chronic leukemias, Leukemia 8 (1994) 990–997.
[19] M. Filipits, G. Pohl, M. Rudas, O. Dietze, S. Lax, R. Grill, et al., Clinical role of multidrug resistance protein 1 expression in chemotherapy resistance in early-stage breast cancer: the Austrian Breast and Colorectal Cancer Study Group, J. Clin. Oncol. 23 (2005) 1161–1168.
[20] K. Nooter, F.T. Bosman, H. Burger, K.E. van Wingerden, M.J. Flens, R.J. Scheper, et al., Expression of the multidrug resistance-associated protein (MRP) gene in primary non-small-cell lung cancer, Ann. Oncol. 7 (1996) 75–81.
[21] G.F. Sullivan, P.S. Amenta, J.D. Villanueva, C.J. Alvarez, J.M. Yang, W.N. Hait, The expression of drug resistance gene products during the progression of human prostate cancer, Clin. Cancer Res. 4 (1998) 1393–1403.
[22] M. Haber, J. Smith, S.B. Bordow, C. Flemming, S.L. Cohn, W.B. London, et al., Association of high-level MRP1 expression with poor clinical outcome in a large prospective study of primary neuroblastoma, J. Clin. Oncol. 24 (2006) 1546–1553.
[23] J. Martin-Broto, A.M. Gutierrez, R.F. Ramos, J.A. Lopez-Guerrero, S. Ferrari, S. Stacchiotti, et al., MRP1 overexpression determines poor prognosis in prospectively treated patients with localized high-risk soft tissue sarcoma of limbs and trunk wall: an ISG/GEIS study, Mol. Cancer Ther. 13 (2014) 249–259.
[24] M.J. Henderson, M. Haber, A. Porro, M.A. Munoz, N. Iraci, C. Xue, et al., ABCC multidrug transporters in childhood neuroblastoma: clinical and biological effects independent of cytotoxic drug efflux, J. Natl. Cancer Inst. 103 (2011) 1236–1251.
[25] K.L. Brouwer, D. Keppler, K.A. Hoffmaster, D.A. Bow, Y. Cheng, Y. Lai, et al., In vitro methods to support transporter evaluation in drug discovery and development, Clin. Pharmacol. Ther. 94 (2013) 95–112.
[26] L. Homolya, M. Hollo, M. Muller, E.B. Mechetner, B. Sarkadi, A new method for a quantitative assessment of P-glycoprotein-related multidrug resistance in tumour cells, Br. J. Cancer 73 (1996) 849–855.
[27] F. Tiberghien, F. Loor, Ranking of P-glycoprotein substrates and inhibitors by a calcein-AM fluorometry screening assay, Anticancer Drugs 7 (1996) 568–578.
[28] C.J. Henrich, H.R. Bokesch, M. Dean, S.E. Bates, R.W. Robey, E.I. Goncharova, et al., A high-throughput cell-based assay for inhibitors of ABCG2 activity, J. Biomol. Screen. 11 (2006) 176–183.
[29] F. Forster, A. Volz, G. Fricker, Compound profiling for ABCC2 (MRP2) using a fluorescent microplate assay system, Eur. J. Pharm. Biopharm. 69 (2008) 396–403.
[30] P.J. Bushway, M. Mercola, J.H. Price, A comparative analysis of standard microtiter plate reading versus imaging in cellular assays, Assay Drug Dev. Technol. 6 (2008) 557–567.
[31] W. Buchser, M. Collins, T. Garyantes, R. Guha, S. Haney, V. Lemmon, et al., Assay development guidelines for image-based high content screening, high content analysis and high content imaging, in: G.S. Sittampalam, N.P. Coussens, H. Nelson, M. Arkin, D. Auld, C. Austin (Eds.), Assay Guidance Manual [Internet], Eli Lilly & Company and the National Center for Advancing Translational Sciences, Bethesda (MD), 2012.
[32] C. Antczak, B. Wee, C. Radu, B. Bhinder, E.C. Holland, H. Djaballah, A high-content assay strategy for the identification and profiling of ABCG2 modulators in live cells, Assay Drug Dev. Technol. 12 (2014) 28–42.
[33] M.R. Ansbro, S. Shukla, S.V. Ambudkar, S.H. Yuspa, L. Li, Screening compounds with a novel high-throughput ABCB1-mediated efflux assay identifies drugs with known therapeutic targets at risk for multidrug resistance interference, PLoS One 8 (2013) e60334.
[34] D.W. Loe, K.C. Almquist, R.G. Deeley, S.P. Cole, Multidrug resistance protein (MRP)-mediated transport of leukotriene C4 and chemotherapeutic agents in membrane vesicles. Demonstration of glutathione-dependent vincristine transport, J. Biol. Chem. 271 (1996) 9675–9682.
[35] I. Leier, G. Jedlitschky, U. Buchholz, S.P. Cole, R.G. Deeley, D. Keppler, The MRP gene encodes an ATP-dependent export pump for leukotriene C4 and structurally related conjugates, J. Biol. Chem. 269 (1994) 27807–27810.
[36] A. Pawarode, S. Shukla, H. Minderman, S.M. Fricke, E.M. Pinder, K.L. O'Loughlin, et al., Differential effects of the immunosuppressive agents cyclosporin A, tacrolimus and sirolimus on drug transport by multidrug resistance proteins, Cancer Chemother. Pharmacol. 60 (2007) 179–188.
[37] J. Wijnholds, G.L. Scheffer, M. van der Valk, P. van der Valk, J.H. Beijnen, R.J. Scheper, et al., Multidrug resistance protein 1 protects the oropharyngeal mucosal layer and the testicular tubules against drug-induced damage, J. Exp. Med. 188 (1998) 797–808.
[38] A. Tamaki, C. Ierano, G. Szakacs, R.W. Robey, S.E. Bates, The controversial role of ABC transporters in clinical oncology, Essays Biochem. 50 (2011) 209–232.
[39] B.C. Shaffer, J.P. Gillet, C. Patel, M.R. Baer, S.E. Bates, M.M. Gottesman, Drug resistance: still a daunting challenge to the successful treatment of AML, Drug Resist. Updat. 15 (2012) 62–69.
[40] M. Kobayashi, H. Saitoh, M. Kobayashi, K. Tadano, Y. Takahashi, T. Hirano, A. Cyclosporin, but not tacrolimus, inhibits the biliary excretion of mycophenolic acid glucuronide possibly mediated by multidrug resistance-associated protein 2 in rats, J. Pharmacol. Exp. Ther. 309 (2004) 1029–1035.
[41] Y.Y. Zaytseva, J.D. Valentino, P. Gulhati, B.M. Evers, mTOR inhibitors in cancer therapy, Cancer Lett. 319 (2012) 1–7.
[42] R. Yuan, A. Kay, W.J. Berg, D. Lebwohl, Targeting tumorigenesis: development and use of mTOR inhibitors in cancer therapy, J. Hematol. Oncol. 2 (2009) 45.
[43] A.S. Don, X.F. Zheng, Recent clinical trials of mTOR-targeted cancer therapies, Rev. Recent Clin. Trials 6 (2011) 24–35.
[44] L.H. Meng, X.F. Zheng, Toward rapamycin analog (rapalog)-based precision cancer therapy, Acta Pharmacol. Sin. 36 (2015) 1163–1169.
[45] L. Ying, Z. Zu-An, L. Qing-Hua, K. Qing-Yan, L. Lei, C. Tao, et al., RAD001 can reverse drug resistance of SGC7901/DDP cells, Tumour Biol. 35 (2014) 9171–9177.
[46] P.L. Tazzari, A. Cappellini, F. Ricci, C. Evangelisti, V. Papa, T. Grafone, et al., Multidrug resistance-associated protein 1 expression is under the control of the phosphoinositide 3 kinase/Akt signal transduction network in human acute myelogenous leukemia blasts, Leukemia 21 (2007) 427–438.
[47] H. Lee, K.H. Jung, Y. Jeong, S. Hong, S.S. Hong, HS-173, a novel phosphatidylinositol 3-kinase (PI3K) inhibitor, has anti-tumor activity through promoting apoptosis and inhibiting angiogenesis, Cancer Lett. 328 (2013) 152–159.
[48] H.B. Jefferies, F.T. Cooke, P. Jat, C. Boucheron, T. Koizumi, M. Hayakawa, et al., A selective PIKfyve inhibitor blocks PtdIns(3,5)P(2) production and disrupts endomembrane transport and retroviral budding, EMBO Rep. 9 (2008) 164–170.
[49] H. Peng, J. Qi, Z. Dong, J.T. Zhang, Dynamic vs static ABCG2 inhibitors to sensitize drug resistant cancer cells, PLoS One 5 (2010) e15276.
[50] E.K. Keeton, K. McEachern, K.S. Dillman, S. Palakurthi, Y. Cao, M.R. Grondine, et al., AZD1208, a potent and selective pan-Pim kinase inhibitor, demonstrates efficacy in preclinical models of acute myeloid leukemia, Blood 123 (2014) 905–913.

[51] M. Haddach, J. Michaux, M.K. Schwaebe, F. Pierre, S.E. O'Brien, C. Borsan, et al., Discovery of CX-6258 a potent, selective, and orally efficacious pan-pim kinases inhibitor, ACS Med. Chem. Lett. 3 (2012) 135–139.
[52] Y. Xie, M. Burcu, D.E. Linn, Y. Qiu, M.R. Baer, Pim-1 kinase protects P-glycoprotein from degradation and enables its glycosylation and cell surface expression, Mol. Pharmacol. 78 (2010) 310–318.
[53] Y. Xie, K. Xu, D.E. Linn, X. Yang, Z. Guo, H. Shimelis, et al., The 44-kDa Pim-1 kinase phosphorylates BCRP/ABCG2 and thereby promotes its multimerization and drug-resistant activity in human prostate cancer cells, J. Biol. Chem. 283 (2008) 3349–3356.
[54] M.T. Huisman, A.A. Chhatta, O. van Tellingen, J.H. Beijnen, A.H. Schinkel, MRP2 (ABCC2) transports taxanes and confers paclitaxel resistance and both processes are stimulated by probenecid, Int. J. Cancer 116 (2005) 824–829.
[55] N. Zelcer, M.T. Huisman, G. Reid, P. Wielinga, P. Breedveld, A. Kuil, et al., Evidence for two interacting ligand binding sites in human multidrug resistance protein 2 (ATP binding cassette C2), J. Biol. Chem. 278 (2003) 23538–23544.
[56] K.M. Hillgren, D. Keppler, A.A. Zur, K.M. Giacomini, B. Stieger, C.E. Cass, et al., Emerging transporters of clinical importance: an update from the international transporter consortium, Clin. Pharmacol. Ther. 94 (2013) 52–63.
[57] H. Kidron, G. Wissel, N. Manevski, M. Hakli, R.A. Ketola, M. Finel, et al., Impact of probe compound in MRP2 vesicular transport assays, Eur. J. Pharm. Sci. 46 (2012) 100–105.
[58] S.H. Iram, S.J. Gruber, D.D. Thomas, S.L. Robia, Structural dynamics of the human MRP1 Drug transporter revealed by intramolecular fluorescence energy transfer, Mol. Pharmacol. 88 (July (1)) (2015) 84–94.